IOPscience iopscience.iop.org

Home Search Collections Journals About Contact us My IOPscience

Multicritical behaviour of disordered Heisenberg antiferromagnets with mixed uniaxial anisotropy

This article has been downloaded from IOPscience. Please scroll down to see the full text article.

1991 J. Phys.: Condens. Matter 3 9733

(http://iopscience.iop.org/0953-8984/3/48/015)

View the table of contents for this issue, or go to the journal homepage for more

Download details:
IP Address: 171.66.16.159
The article was downloaded on 12/05/2010 at 10:55

Please note that terms and conditions apply.

J. Phys.: Condens. Matter 3 (1991) 9733–9739. Printed in the UK

Multicritical behaviour of disordered Heisenberg antiferromagnets with mixed uniaxial anisotropy

J Seier, K D Usadel and A Moschel
Theoretische Tieftemperaturphysik, Universität Duisburg, Lotharstrasse 1, 4100 Duisburg 1, Federal Republic of Germany

Received 18 January 1991

Abstract. Magnetic phase diagrams of disordered Heisenberg antiferromagnets with mixed uniaxial anisotropy are calculated within a local molecular field theory. The phase diagrams numerically obtained for sets of parameters relevant for the system $Fe_{1-x}Ni_xCl_2$ are in very good agreement with recent experimental results. It is demonstrated that by changing the concentration x, or the ratio of the anisotropies, a rich variety in the physical behaviour of these systems can be expected.

1. Introduction

Antiferromagnets with uniaxial anisotropy show a rich variety of different phases in their H versus T phase diagrams. These systems have been investigated theoretically in a number of papers [1–3]. Experimentally, special interest has been focused on the extreme cases of both strong and weak anisotropy [4, 5]. Of particular interest, however, is the case of an intermediate uniaxial anisotropy where, according to an investigation of Vilfan and Galam [3], a bicritical point (BCP) and a tricritical point (TCP) merge resulting in a new multicritical point. It was suggested [6] that a system with intermediate anisotropy can be obtained experimentally by alloying systems with extreme anisotropies. Recently these experiments have been carried out. In [7] the system $Fe_{1-x}Ni_xCl_2$ was investigated in the concentration range $0.18 \leqslant x \leqslant 0.67$. These experiments confirm the scenario of multicritical behaviour in antiferromagnets with intermediate uniaxial anisotropy put forward by Vilfan and Galam.

In [6] a comparison of experimental results with theoretical calculations has been carried out using a virtual crystal approximation (VCA) for the mixed system $Fe_{0.5}Ni_{0.5}Cl_2$. In this approximation the exchange constants as well as the single-ion anisotropy constants are averaged resulting in a translational invariant Hamiltonian which has been investigated earlier within a molecular field approximation [3].

A virtual crystal approximation although certainly being a valid first step in a theoretical investigation has, however, some severe drawbacks as can be seen in the following. If one considers two types of ions with equal concentration and strong anisotropies, which have equal absolute values but different signs, the averaged anisotropy vanishes although the system is strongly disordered. Therefore it is necessary and very interesting to go beyond the VCA. In the present paper, we investigate a Heisenberg antiferromagnet with mixed uniaxial anisotropy. We consider a random mixture of two types of magnetic

0953-8984/91/489733 + 07 $03.50 © 1991 IOP Publishing Ltd

ions having both equal spin $S = 1$. Exchange interactions J, anisotropy constants D and Landé-factors g are ion dependent. The system is treated within a local molecular field approximation (MFA). In some of our numerical calculations we use parameters obtained experimentally for the systems $FeCl_2$ and $NiCl_2$, respectively, so that for the mixed system $Fe_{1-x}Ni_xCl_2$ a direct comparison with experimental work becomes possible.

2. Outline of the calculations

For each lattice site l we introduce a quantity K_l, which is either equal to one with probability x, i.e. the probability that a site l is occupied with a Ni-atom; or which is equal to zero with probability $1 - x$, i.e. the probability that a site l is occupied with a Fe-atom. Then the molecular field acting on a Ni-atom on site l' is given by:

$$\underline{\Delta}_{l'}^{a}(\mathrm{Ni}) = g_{\mathrm{Ni}}\underline{H} - \sum_{l} (J_{\mathrm{Ni,Ni}}^{\mathrm{AF}} K_l + J_{\mathrm{Ni,Fe}}^{\mathrm{AF}}(1 - K_l))\langle \underline{S}\rangle_{\mathrm{b}}$$

$$+ \sum_{l} (J_{\mathrm{Ni,Ni}}^{\mathrm{FM}} K_l + J_{\mathrm{Ni,Fe}}^{\mathrm{FM}}(1 - K_l))\langle \underline{S}\rangle_{\mathrm{a}}. \tag{1}$$

The indices a and b label the two sublattices. Of course, similar equations hold for Ni-atoms at a b-site and for Fe-atoms sitting either at an a-site or a b-site. The spin expectation values $\langle \underline{S}\rangle$ are assumed to be averaged quantities having two values depending on whether the spin is sitting on an a-site or a b-site, respectively.

In the special case of $Fe_{1-x}Ni_xCl_2$ each magnetic ion has six neighbours which are coupled to it ferromagnetically and six neighbours with antiferromagnetic coupling. For the sake of a comparison with experiments all these interactions are included in (1). Of course, one can think about slightly simpler molecular field equations for model systems. But since the final calculations have to be done numerically, the inclusion of all terms relevant to a certain system does not make a great difference. It has, of course, the advantage, that a direct comparison with experimental results is possible.

Treating the spin as a quantum object with $S = 1$ the free energy of a certain spatial configuration of magnetic ions is calculated under the influence of local exchange and anisotropy fields. Since each magnetic ion has six antiferromagnetically and six ferromagnetically coupled neighbours, there are 49 possibilities of occupying those places with Fe or Ni atoms. Averaging over all configurations yields the free energy per spin. The calculation is rather tedious but, in principle, straightforward. In the antiferromagnetic phase we obtain

$$\frac{F_{\mathrm{AF}}}{N} = -\bar{\delta}m^2 + \bar{\delta}m_s^2 - k_{\mathrm{B}}T\sum_{i,j}\binom{6}{i}\binom{6}{j}x^{i+j}(1-x)^{12-i-j}$$

$$\times \{x \ln[1 + 2\mathrm{e}^{\beta D_1}\cosh\beta\Lambda_{1p}(i,j)]$$

$$+ x \ln[1 + 2\mathrm{e}^{\beta D_1}\cosh\beta\Lambda_{1m}(i,j)]$$

$$+ (1-x)\ln[1 + 2\mathrm{e}^{\beta D_2}\cosh\beta\Lambda_{2p}(i,j)]$$

$$+ (1-x)\ln[1 + 2\mathrm{e}^{\beta D_2}\cosh\beta\Lambda_{2m}(i,j)]\} \tag{2}$$

with

$$\bar{\delta} = x^2 J^{AF}_{Ni,Ni} + 2x(1-x)J^{AF}_{Fe,Ni} + (1-x)^2 J^{AF}_{Fe,Fe} - x^2 J^{FM}_{Ni,Ni} - 2x(1-x)J^{FM}_{Fe,Ni} - (1-x)^2 J^{FM}_{Fe,Fe} \tag{3}$$

and

$$\bar{\gamma} = x^2 J^{AF}_{Ni,Ni} + 2x(1-x)J^{AF}_{Fe,Ni} + (1-x)^2 J^{AF}_{Fe,Fe} + x^2 J^{FM}_{Ni,Ni} + 2x(1-x)J^{FM}_{Fe,Ni} + (1-x)^2 J^{FM}_{Fe,Fe}. \tag{4}$$

The local fields appearing in the free energy are given by the following set of equations:

$$\begin{aligned}
\Lambda_{1p}(i,j) &= g_{Ni}H - \delta_1(i,j)m + \gamma_1(i,j)m_s \\
\Lambda_{1m}(i,j) &= g_{Ni}H - \delta_1(i,j)m - \gamma_1(i,j)m_s \\
\Lambda_{2p}(i,j) &= g_{Fe}H - \delta_2(i,j)m + \gamma_2(i,j)m_s \\
\Lambda_{2m}(i,j) &= g_{Fe}H - \delta_2(i,j)m - \gamma_2(i,j)m_s \\
\delta_1(i,j) &= iJ^{AF}_{Ni,Ni} + (6-i)J^{AF}_{Fe,Ni} - jJ^{FM}_{Ni,Ni} - (6-j)J^{FM}_{Fe,Ni} \\
\delta_2(i,j) &= iJ^{AF}_{Fe,Fe} + (6-i)J^{AF}_{Fe,Ni} - jJ^{FM}_{Fe,Fe} - (6-j)J^{FM}_{Fe,Ni} \\
\gamma_1(i,j) &= iJ^{AF}_{Ni,Ni} + (6-i)J^{AF}_{Fe,Ni} + jJ^{FM}_{Ni,Ni} + (6-j)J^{FM}_{Fe,Ni} \\
\gamma_2(i,j) &= iJ^{AF}_{Fe,Fe} + (6-i)J^{AF}_{Fe,Ni} + jJ^{FM}_{Fe,Fe} + (6-j)J^{FM}_{Fe,Ni}.
\end{aligned} \tag{5}$$

In these equations m denotes the homogeneous magnetization $m = \frac{1}{2}(\langle S_{az}\rangle + \langle S_{bz}\rangle)$, while m_s is the staggered magnetization $m_s = \frac{1}{2}(\langle S_{az}\rangle - \langle S_{bz}\rangle)$, both in the z-direction. The indices i and j, referring to the antiferromagnetically and ferromagnetically coupled neighbours respectively, run from 0 to 6.

In the spin–flop phase m_s is zero, but now the order parameter $m_\perp = \frac{1}{2}(\langle S_{ax}\rangle - \langle S_{bx}\rangle)$ has a finite value. The corresponding free energy in this phase reads:

$$\frac{F_{SF}}{N} = -\bar{\delta}m^2 + \bar{\gamma}m_\perp^2 - 2k_B T \sum_{i,j} \binom{6}{i}\binom{6}{j} x^{i+j}(1-x)^{12-i-j} \times [x \ln(e^{-\beta\lambda_1^{(1)}} + e^{-\beta\lambda_2^{(1)}} + e^{-\beta\lambda_3^{(1)}}) + (1-x)\ln(e^{-\beta\lambda_1^{(2)}} + e^{-\beta\lambda_2^{(2)}} + e^{-\beta\lambda_3^{(2)}})]. \tag{6}$$

The $\lambda_k^{(l)}$ are the eigenvalues of a matrix already derived in an earlier paper by Vilfan and Žekš [2], and are given by:

$$\lambda_k^{(l)} = (2/\sqrt{3})[\tfrac{1}{3}D_l^2 + \Lambda_{xl}^2(i,j) + \Lambda_{zl}^2(i,j)]^{1/2} \cos(\varphi_l/3 + k\,2\pi/3) - \tfrac{2}{3}D_l \tag{7}$$

with

$$\cos\varphi_l = (\sqrt{3}/2)D_l\,[\tfrac{2}{3}D_l^2 + \Lambda_{xl}^2(i,j) - 2\Lambda_{zl}^2(i,j)]/[\tfrac{1}{3}D_l^2 + \Lambda_{xl}^2(i,j) + \Lambda_{zl}^2(i,j)]^{3/2}. \tag{8}$$

The index l takes the value 1 for a Ni-atom and 2 for a Fe-atom. In the spin–flop phase

Table 1. Parameters obtained experimentally for the systems $FeCl_2$ and $NiCl_2$ [4, 5], k_B denotes the Boltzmann constant.

Parameter	$FeCl_2$	$NiCl_2$
S	1	1
J^{AF}/k_BK	0.18	0.77
J^{FM}/k_BK	3.94	21.7
D/k_BK	9.8	−0.4
g	4.1	2.2

the molecular fields of both sublattices differ only in the sign of their x-components. With $\Lambda_{ax} = -\Lambda_{bx} = \Lambda_x$ and $\Lambda_{az} = \Lambda_{bz} = \Lambda_z$ they read

$$\Lambda_{xl}(i,j) = -\gamma_l(i,j)m^{\perp} \tag{9}$$

and

$$\Lambda_{zl}(i,j) = g_lH - \delta_l(i,j)m. \tag{10}$$

The averaged molecular field equations can now be evaluated with methods discussed in detail in the paper of Vilfan and Žekš [2]. In the next section we shall present some of our results.

3. Results and discussion

In figure 1 we show three phase diagrams obtained for parameters which correspond to the system $Fe_{1-x}Ni_xCl_2$. We used parameters obtained experimentally for the pure systems $FeCl_2$ and $NiCl_2$ [4, 5]. They are listed in table 1. The exchange constant between Ni and Fe in $Fe_{1-x}Ni_xCl_2$ is not known, so we decided to use the mean value $J_{Fe,Ni} = \frac{1}{2}(J_{Fe,Fe} + J_{Ni,Ni})$.

In figure 1 the calculated phase diagram for the system $Fe_{0.5}Ni_{0.5}Cl_2$ is shown (upper curve). In agreement with the experimental phase diagram obtained in [6] we found a spin–flop (SF) phase ending in a critical endpoint (CEP), a phase transition between paramagnetic (PM) and antiferromagnetic (AF) phase of first order between a CEP and a TCP and a second order transition between the TCP and the Néel-temperature $T_N(x = 0.5) = 48.9$ K. The corresponding experimental value is $T_N = 40.9$ K [6]. Note, however, that the experimental values for the CEP and the TCP are significantly lower than those we obtained. Note also that the VCA using the same parameters as we did does not give a spin–flop phase.

The SF phase obtained for $Fe_{0.5}Ni_{0.5}Cl_2$ is only stable between the CEP and a second CEP at a lower temperature $T = 0.4\,T_N$. This interesting behaviour has not yet been found neither in the experiments on $Fe_{0.5}Ni_{0.5}Cl_2$ [6] nor in those on $Fe_{1-x}Ni_xCl_2$ for the concentrations x investigated in [7]. In our calculations the second CEP at lower temperatures $T > 0$ appears only in a rather narrow range of concentrations: $0.358 < x < 0.56$. Above $x = 0.56$ the SF phase is stable down to $T = 0$.

By increasing the concentration x the CEP approaches the TCP. They merge at $x_c = 0.64$ forming the multicritical point as predicted by Vilfan and Galam [3]. This again is in very good agreement with experiments, the corresponding experimental value is $x_c =$

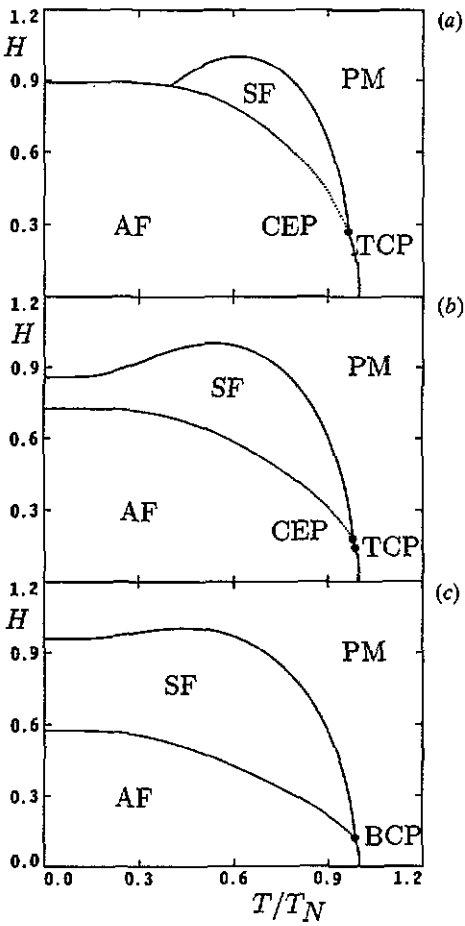

Figure 1. Calculated phase diagrams of $Fe_{1-x}Ni_xCl_2$ for different values of x. From the top: $x = 0.5, 0.6, 0.7$. Temperature is measured relative to the Néel temperature T_N, and magnetic field H in arbitrary units. The Néel temperatures are (*a*) $T_N(x = 0.5) = 48.9$ K, (*b*) $T_N(x = 0.6) = 53.5$ K and (*c*) $T_N(x = 0.7) = 57.9$ K.

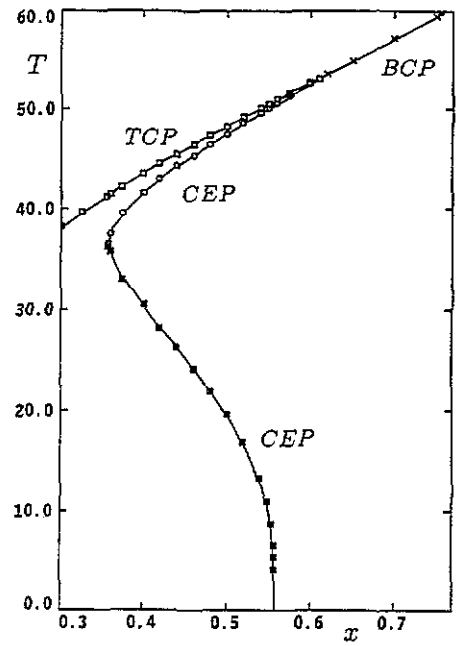

Figure 2. x–T phase diagram of $Fe_{1-x}Ni_xCl_2$. Temperature is measured in K. ×, the BCP; □, the TCP; ○, the upper CEP; and ■, the lower CEP.

0.57 [7]. For $x \geq 0.7$ the mixed system shows a behaviour similar to a pure antiferromagnet with weak uniaxial anisotropy, i.e. it possesses a BCP instead of a TCP.

Decreasing the concentration x the width of the spin–flop phase decreases rapidly and it vanishes at $x = 0.358$. The upper CEP and the TCP both decrease and the latter approaches a finite value for $x \to 0$. These results are summarized in figure 2 where the most interesting part of the x–T phase diagram is shown.

For other sets of parameters a variety of different phase diagrams has been calculated numerically and not all of them can be shown here of course. Rather, in the following we would like to concentrate on one issue, namely the dependence of the phase diagrams on the anisotropies D_1 and D_2. In model calculations we used a fixed mean value $\bar{D} =$

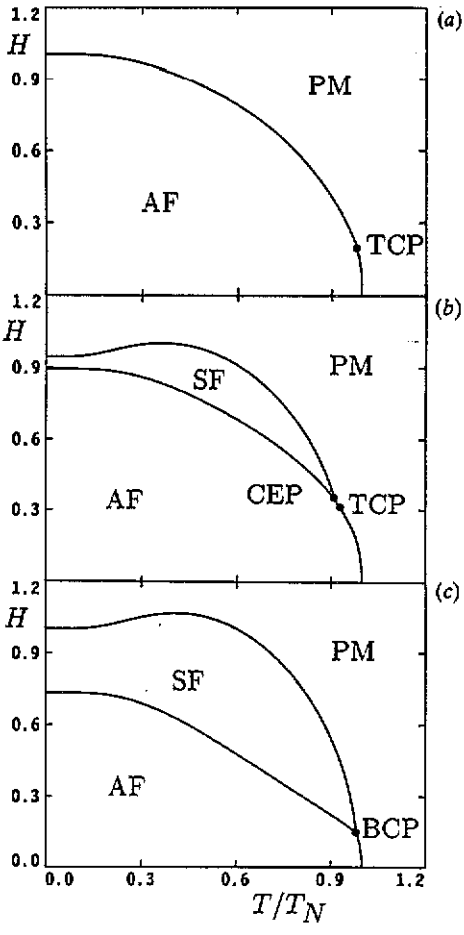

Figure 3. Phase diagrams of model systems with different values of uniaxial anisotropies. (*a*) $D_1 = D_2 = 5$, (*b*) $D_1 = 2$, $D_2 = 8$ and (*c*) $D_1 = -1$, $D_2 = 11$. Units are the same as in figure 1.

$\frac{1}{2}(D_1 + D_2)$ as well as fixed exchange constants and a fixed concentration of $x = 0.5$ varying only the ratio D_1/D_2. For the antiferromagnetic couplings between each type of ions we used $0.5\,k_BK$ and $1.0\,k_BK$, respectively, and $0.2\,k_BK$ and $1.0\,k_BK$ for the ferromagnetic couplings. The results are shown in figure 3.

For $D_1 = D_2 = 5$ a TCP is obtained, but there is no stable SF phase. This corresponds to a system with a strong uniaxial anisotropy, e.g. confirmed experimentally for $FeCl_2$ [4]. A reduction of D_1 leads to the appearance of a spin–flop phase. For $D_2 > D_1 > 0$ one obtains a CEP and a TCP with a distance decreasing with decreasing D_1. For $D_1 < 0$ a BCP appears instead of a CEP and a TCP. The change from tricritical to bicritical behaviour is very similar to the behaviour found for the system $Fe_{1-x}Ni_xCl_2$ by changing the concentration instead of the anisotropy constants.

4. Conclusion

The detailed investigation of disordered systems using a local molecular field approximation leads to a substantial improvement of the theoretical results as compared with

results obtained within a VCA. Qualitative agreement with experimental results is obtained and even quantitatively the agreement is rather satisfying. The reason might be the large number of neighbours in the system studied, which has a tendency to improve the accuracy of the molecular field theory.

Acknowledgments

This work was supported by the Deutsche Forschungsgemeinschaft through Sonderforschungsbereich 166. The authors thank W Kleemann and E Cleve for making available their experimental results prior to publication.

References

[1] Kincaid J M and Cohen E G D 1975 *Phys. Rep.* **22** 57
[2] Vilfan I and Žekš B 1979 *J. Phys. C: Solid State Phys.* **12** 4295
[3] Vilfan I and Galam S 1986 *Phys. Rev.* B **34** 6428
[4] Dillon J F, Chen E Y and Guggenheim H J 1978 *Phys. Rev.* B **18** 377
[5] Lindgard P A, Birgeneau R J, Als-Nielsen J and Guggenheim H J 1975 *J. Phys. C: Solid State Phys.* **8** 1059
[6] Igel B, Kleemann W and Vilfan I 1990 *J. Phys.: Condens. Matter* **2** 4495
[7] Cleve E and Kleemann W 1991 *Phase Transitions* submitted